PRECISION CLOSED-LOOP ORBITAL MANEUVERING SYSTEM DESIGN AND PERFORMANCE FOR THE MAGNETOSPHERIC MULTISCALE FORMATION

Dean J. Chai[(1)], **Steven Z. Queen**[(2)], **and Samuel J. Placanica**[(3)]
[(1)]*NASA GSFC, Greenbelt, MD, USA, 301-286-2629, dean.j.chai@nasa.gov*
[(2)]*NASA GSFC, Greenbelt, MD, USA, 301-286-0988, steven.z.queen@nasa.gov*
[(3)]*NASA GSFC, Greenbelt, MD, USA, 301-286-8836, samuel.j.placanica@nasa.gov*

Abstract: *NASA's Magnetospheric MultiScale (MMS) mission successfully launched on March 13, 2015 (UTC) consists of four identically instrumented spin-stabilized observatories that function as a constellation to study magnetic reconnection in space. The need to maintain sufficiently accurate spatial and temporal formation resolution of the observatories must be balanced against the logistical constraints of executing overly-frequent maneuvers on a small fleet of spacecraft. These two considerations make for an extremely challenging maneuver design problem. This paper focuses on the design elements of a 6-DOF spacecraft attitude control and maneuvering system capable of delivering the high-precision adjustments required by the formation designers—specifically, the design, implementation, and on-orbit performance of the closed-loop "formation-class" maneuvers that include initialization, maintenance, and re-sizing. The maneuvering control system flown on MMS utilizes a micro-gravity resolution accelerometer sampled at a high rate in order to achieve closed-loop velocity tracking of an inertial target with arc-minute directional and millimeter-per-second magnitude accuracy. This paper summarizes the techniques used for correcting bias drift, sensor-head offsets, and centripetal aliasing in the acceleration measurements. It also discusses the on-board pre-maneuver calibration and compensation algorithms as well as the implementation of the post-maneuver attitude adjustments.*

Keywords: *Formation flying, maneuver/attitude dynamics, determination and control.*

1. Introduction

The Magnetospheric MultiScale (MMS) mission, launched on March 13, 2015 (UTC), is the fourth mission of NASA's Solar Terrestrial Probe program. The MMS mission consists of four identically instrumented observatories that function as a constellation to provide the first definitive study of magnetic reconnection in space. Since it is frequently desirable to isolate electric and magnetic field sensors from stray effects caused by the spacecraft's core body, the suite of instruments on MMS includes six radial and two axial instrument booms with deployed lengths ranging from 5–60 meters (see Fig. 1). The observatory is spin stabilized about its positive z-axis with a nominal rate slightly above three revolutions per minute (RPM). The spin is primarily used to maintain tension in the four radial wire booms.

Each observatory's Attitude Control System (ACS) consists of two digital sun sensors, four star camera heads, one three-axis accelerometer, and twelve mono-propellant hydrazine thrusters—responsible for orbital adjustments, attitude control, and spin adjustments. Prior to the establishment of the formation, each MMS observatory underwent commissioning activities during the first 90 days of the mission. However, the majority of the commissioning-phase milestones—which included events such as boom deployments, slews to mission attitude, open-loop perigee raising

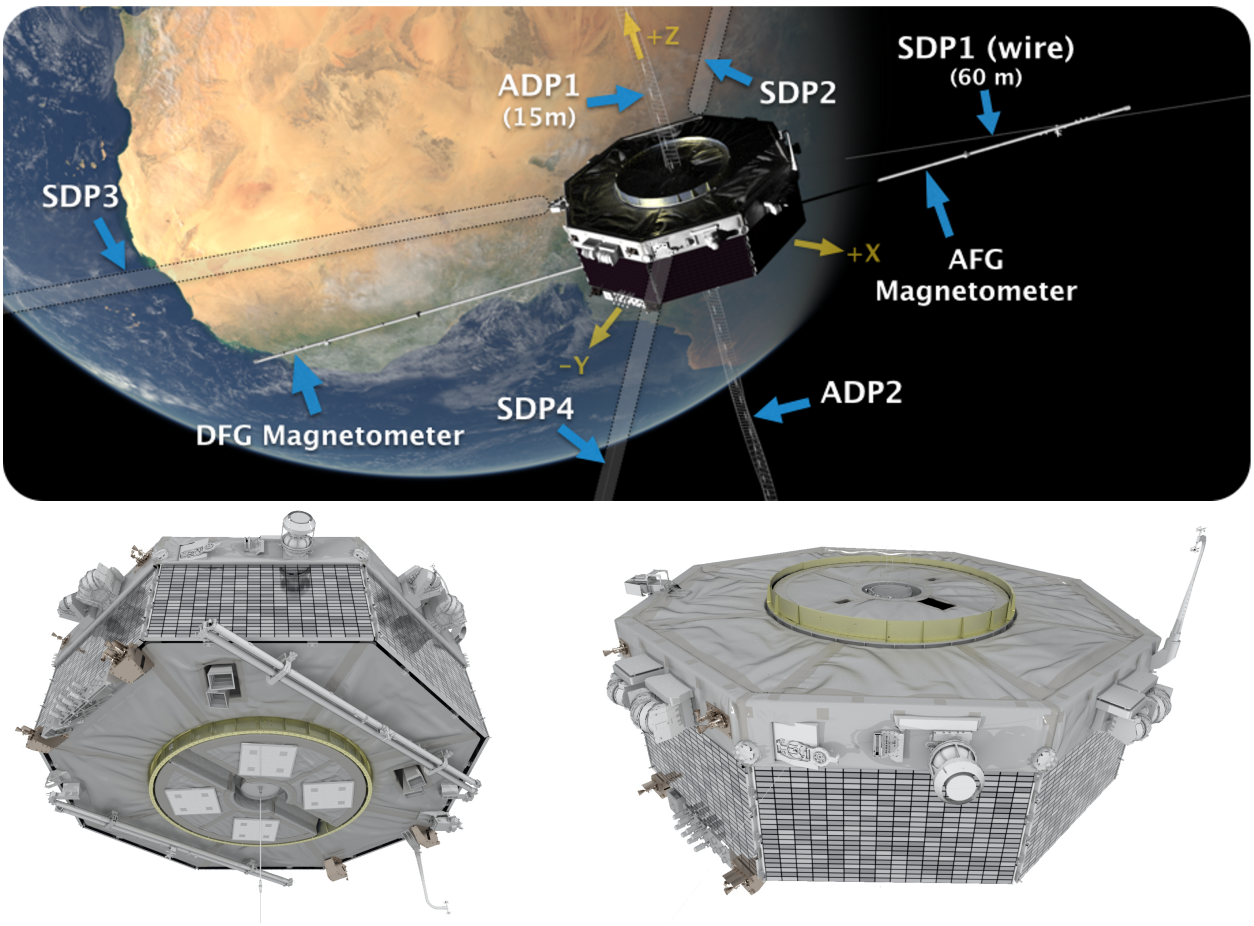

Figure 1. MMS Observatory (Stowed / Fully-Deployed)

maneuvers, and instrument calibration slews—are not the emphasis of this paper. Instead, the current text focuses on the "formation-class" of maneuvers executed while the observatories are in their fully deployed configuration. The formation maneuvers were by far the most challenging of the MMS mission-design, and had been the motivation for the accelerometer feedback-driven translational controller design (a.k.a. *closed-loop "delta-V"*). Extensive Monte Carlo analysis methods were required to demonstrate the on-board system's robustness and ability to meet the stringent performance demands.

The sections that follow describe the spacecraft configuration, performance requirements, hardware, and algorithms used for 6-DOF estimation and control, and the final formation maneuver sequence design. The paper concludes with maneuver performance based on both simulated and on-orbit telemetry.

1.1. Spacecraft Configuration

Compounding some of the difficulties with precise pointing and maneuvering is the arrangement of the MMS instrument suite. The observatories consist of eight independent deployable booms—six radial and two axial—the most striking of which are the four symmetric Spin-plane Double Probes

(SDP) deployed on independent 60-meter tethers. The SDP utilizes the gyrodynamics of spacecraft spin (nominally 3.1 RPM) to both deploy and maintain their relative positions. Furthermore, there is a retractable element in the SDP design such that a minimum tension of 0.51 N must be maintained at about 57 meters outboard from the base body attachment point at all times including during maneuvers. The minimum tension requirement was the reason why MMS mission increased its initial nominal spin rate from 3.0 RPM to 3.1 RPM.

The two 15-meter Axial Double Probe (ADP) booms are mounted at the observatory's geometric center on the X-Y plane, one on each of the top and bottom decks. ADP booms excitation are primarily due to radial thrusting. There is a concern that ADP root-bending moment could exceed its design specification due to controller-induced resonance. Since there is no real-time feedback measurement available in flight to warn of impending failure, the simulated ADP root-bending moment is monitored closely during the design process. The control systems is designed so that there are no occurrences of ADP root-bending moment exceeding its design limits (with margin) at any point in any of the Monte Carlo simulation-ensembles used to validate maneuvers.

Table 1. Observatory Maneuver Safety Constraints

Safety Constraints	**Limits**
SDP In-plane Deflection	$< 14^\circ$
SDP Out-of-plane Deflection	$< 7^\circ$
SDP Tension at Retraction Point of Interest	> 0.51 N
SDP and Magnetometer Boom Separation Distance	> 1.0 m
ADP Root Bending Moment	< 14.3 N-m

The other two radial booms are the 5-meter (rigid) magnetometer booms. They are aligned 180 degrees apart and are about 30 degrees from the closest pair of the SDP booms. However, they are mounted on the bottom deck of the spacecraft rather than the top deck where all the other science instruments are located. In order to prevent possible entanglement between magnetometer booms and SDP booms, safety constraints including maximum deflection angles and minimum separation are strictly enforced during the design process. All of the critical observatory maneuver safety constraints are summarized in Tab. 1.

1.2. Formation Maneuver Performance Requirements

Once in stable science-gathering orbits, the four fully deployed observatories form a tetrahedron with as little as 4-km of separation between spacecraft. The need to maintain a sufficiently accurate spatial and temporal formation must be balanced against the logistical constraints of executing overly-frequent maneuvers on a fleet of spacecraft. These two considerations make for an extremely challenging orbit design problem[1, 2].

With a stated operational goal of maneuvering the fleet no more often than once every two weeks (on average), MMS flight dynamics specialists devised the "1%" maneuver magnitude error requirement for all formation-type maneuvers. The requirements were refined after preliminary Monte Carlo simulation results revealed accuracy limitations for the very small maneuvers. The final maneuver

Table 2. Formation Maneuver Performance Requirements

Maneuver Size	**Error Allocation** (3σ)	
(m/sec)	Magnitude	Direction*
0.00 – 0.10	5 mm/sec	$40^\circ \rightarrow 5^\circ$
0.10 – 0.50	5 mm/sec	$5^\circ \rightarrow 1.5^\circ$
> 0.50	1%	1.5°

* ($\rightarrow$ indicates linear decrease vs. size)

requirements include an absolute magnitude floor as well as some relief on the directional errors for the smaller formation maneuvers (see Tab. 2). Operationally, the flight dynamics team evaluates the "pros" and "cons" of performing these very small maneuvers during the planning phase of a maneuver. It is conceivable that the flight dynamic team would "wave off" a maneuver—or a set of maneuvers—for the entire fleet based on their assessment of the trade-offs.

1.3. Controls Sensors and Actuators

Each MMS observatory is equipped with a μASC Star Tracker System (STS), two Digital Sun Sensors (DSS), an Acceleration Measurement System (AMS), a Goddard Global Positioning System Receiver (Navigator), and twelve hydrazine mono-propellant thrusters. STS and AMS are the primary closed-loop feedback sensors. DSS is only used in the Sun Acquisition Mode algorithm. Navigator is used for the "quick-look" maneuver assessment after each maneuver and the refined definitive orbit solution processed by the ground.

1.3.1. Star Tracker and Onboard Attitude Estimate

The μASC Star Tracker System, provided by the Technical University of Denmark, consists of internally redundant electronics housed within a single enclosure that interfaces with four Charge-Coupled Device camera head units. The STS provides time-stamped attitude quaternion data packets at a 4 Hz telemetry rate. It has a 3σ full performance transverse and bore-sight axis accuracy of 60 and 200 arcsec, respectively. The STS has a spin rate capability of up to 4 RPM. Figure 2 shows a 752×580 pixel image taken on April 27, 2015 by Observatory 3 (MMS-3) using STS camera head unit B.

The raw measurements from all four star sensor camera-head units (CHU) are combined using a Multiplicative Extended Kalman Filter (MEKF). Due to limitations in the processing power of the flight computer (Motorola RH-CF5208 Coldfire), neither the sun sensor nor the acceleration measurements are included in the filter's computations. A detailed description of the MMS MEKF implementation has been summarized in [3], and is also included in a more general MMS system identification paper at this conference[4].

1.3.2. Accelerometer and Acceleration Feedback Processing

The Acceleration Measurement System was manufactured by ZIN Technologies (Cleveland, Ohio). It provides three-axis acceleration measurements during orbit adjustments and integrates these

Figure 2. DTU μASC Image (OBS 3, CHU B)

samples in order to help determine the net velocity change (Δv) imparted by these maneuvers. The AMS incorporates internally redundant electronics within a single enclosure with each side interfacing with its own set of three single-axis orthogonally mounted Honeywell QA3000 accelerometer sensors. The AMS electronics include high-rate (100 kHz) analog-to-digital signal conversion. An embedded processor down samples and filters the acceleration data. The AMS has a dynamic range of greater than $\pm$25,000 μg, a resolution of less than 1 μg, a short-term, 1σ bias stability over a twelve hour period of better than 1 μg, and an effective bandwidth of 250 Hz.

The quantity of interest from a formation-maintenance perspective is not the acceleration *per se*, but the change in velocity of the spacecraft's center-of-mass (CM) due to thrusting. Analogous to a rate-integrating gyro for attitude dynamics, the AMS's primary function for the mission is to act as an acceleration-integrating accelerometer during orbital-adjustments. The true imparted $\Delta\mathbf{v}_c$ that we control over the time interval (t_1, t_2) and its relationship with the AMS measurement is summarized by this general equation derived and explained in [3].

$$\underbrace{\Delta\mathbf{v}_c(t_1,t_2)}_{\text{truth states}} = \underbrace{\int_{t_1}^{t_2} \underset{i\leftarrow b}{\mathcal{A}}\, \mathbf{a}_k\, d\tau}_{\text{measurement}} + \underbrace{\left\{ \underset{i\leftarrow b}{\mathcal{A}}\, \boldsymbol{\omega}^{\times}\mathbf{r}_{cd} \right.}_{\text{centripetal}} \underbrace{- \left. \underset{i\leftarrow b}{\mathcal{A}}\, \dot{\mathbf{r}}_c \right\}_{t_1}^{t_2}}_{\text{multi-body}} \underbrace{- \int_{t_1}^{t_2} \underset{i\leftarrow b}{\mathcal{A}}\, \mathbf{b}\, d\tau}_{\text{bias}} \underbrace{- \int_{t_1}^{t_2} \underset{i\leftarrow b}{\mathcal{A}}\, \eta\, d\tau}_{\text{noise}} \tag{1}$$

where the symbol $\mathcal{A}$ is the direction-cosine matrix transformation from the body-fixed to inertial

frame, $\mathbf{a}_k$ is the sampled acceleration in the body-fixed frame, ω is angular rate expressed in body-fixed coordinates, $\mathbf{r}_{cd}$ is the position vector from the base-body's CM to the accelerometer head expressed in the body-fixed frame, $\mathbf{r}_c$ is the position of the base-body's CM expressed in the body-fixed frame. b and η are intrinsic electro-mechanical bias vector and sensor noise vector (also expressed in the body-fixed frame).

The first term on the right-hand side of Eq. (1), the measurement integral, is obtained by sampling the analog accelerometer (e.g. QA 3000) at a sufficiently high rate to capture all the relevant dynamics of the maneuvering spacecraft. In the case of MMS, the AMS electronics samples well above 1 kHz, and then applies appropriate decimation, anti-aliasing, and noise reduction filters to deliver a "clean" 1 kHz digital signal. The discrete AMS output has a bandwidth of 250 Hz, and less than ± 5 ppm of gain and/or $\pm 1^\circ$ of phase distortion in the pass-band. Since the MMS ACS operates on a 4 Hz control cycle, the measurement integral contains 250 subsamples that are combined with frame rotation compensation[3] internal to the AMS in order to output a single velocity-increment.

In the ACS flight software outside of the AMS, the sub-interval sample is transformed into the inertial frame, and centripetal compensation is performed before summation to produce the total maneuver velocity-change estimate for closed-loop control. The multi-body term is not compensated specifically via on-board algorithm; however, it has been demonstrated by Monte Carlo method that the multi-body term will—over a sufficiently long interval—integrate to zero, and therefore would have no effect on base body CM motion, $\Delta\mathbf{v}_c$. The bias term is compensated via a two-step pre-maneuver calibration scheme. And finally, the AMS noise characteristics are such that the integrated noise is well within the closed-loop requirements. All of these the above effects and other errors are detailed in [3].

1.3.3. Thrusters and Pulse-Width Modulation

Both the attitude and orbital control of the observatories is accomplished using twelve hydrazine mono-propellant thrusters (Fig. 3)—four AMPAC 1-lbf (4.4 N) thrusters are directed axially ($\pm$z) and eight Aerojet 4-lbf (17.8 N) thrusters radially ($\pm$y). The minimum impulse bit for the Aerojet designed thrusters ranges throughout the mission from 0.13–0.26 N-m-sec, which corresponds to a 20 millisecond pulse.

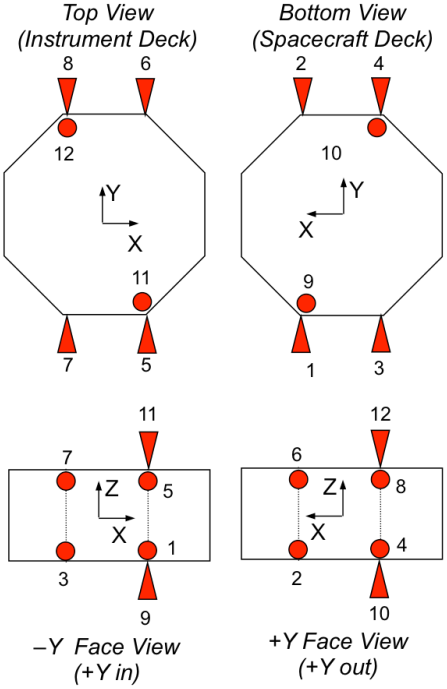

Figure 3. MMS Thruster Layout

In addition to a continuous firing mode, the engine-value driver (EVD) is capable of modulating the duty cycle of the output on 8 Hz boundaries. Only, the radial thrusters are modulated when used in translational control. Each radial thruster is assigned a duty-cycle based on ground knowledge of the overall spacecraft mass properties, its calibrated thrust value, and planned pairs with other thrusters. Th notional goal is to minimizing disturbance torques for pure translational control. However, the on-board system does not dynamically adjust thruster duty-cycles during a maneuver (other than by complete off-pulsing as discussed

later). The interleaved momentum control (see section 3.2.3.) is sufficient to cancel induced rate errors and maintain attitude. The MMS ground calibration methods[4][5] in combination with a diaphragm-ed tank design are sufficient for the ACS to meet its performance requirements—without resorting to the dynamic manipulation of duty-cycles.

2. Formation Maneuver Sequence

A MMS formation maneuver consists a pre-maneuver principal axis calibration, a pre-maneuver accelerometer bias calibration, a translational control ("delta-V") maneuver, and a momentum control ("delta-H") maneuver (Fig. 4).

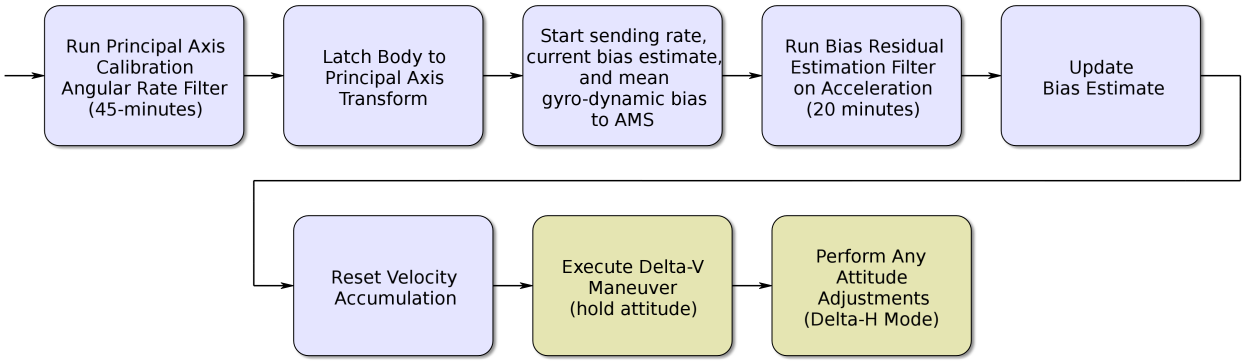

Figure 4. Closed-loop Delta-V (Formation) Maneuver Template

A MMS formation maneuver sequence is made up of six formation maneuvers—two for each of three spacecraft—and one momentum control delta-H maneuver for the remaining reference observatory. The first set of three formation maneuvers in a sequence is commonly referred to as FM1, the first of a pair of delta-V maneuvers to start the relative motion necessary to attain the desirable formation. The second set of a pair of delta-V maneuvers (FM2) is meant for stopping the designed relative motion in preparation for establishing a good formation tetrahedron in the science region of interest (ROI). The delta-H maneuvers are used to keep the spacecraft momentum at the desirable science attitude. The three observatories performing the formation maneuvers would each perform half of the desirable attitude slew during FM1 and FM2. The reference spacecraft would only slew towards its attitude target while the other three are performing their FM1, and not maneuver at all while the others are performing FM2. The reasoning behind this approach is that—if the reference spacecraft's orbit was perturbed—the planned FM1 can proceed as normal. The flight dynamics planners then preserve the option to re-plan FM2 maneuvers to "formation-fly" around the slightly perturbed reference spacecraft. In flight, the orbit perturbations due to attitude slew maneuvers have been observed to be benign, so no FM2 re-plans have been required.

3. MMS Delta-V Controller Design

The MMS Delta-V Controller controls all 6 degrees of freedom (6-DOF). However, instead of adopting a general 6-DOF control law, the controller has separate logic for velocity control and momentum control. Since thrusters are the only actuators available, the two control laws and their respective thruster commands are processed independently and are on separate schedules. This

approach avoided the need to implement a novel 6-DOF controller on a spin-stabilized spacecraft with long appendages, while also introducing some performance limitations. The following sections cover the controller logic in greater detail—including features implemented later in the design phase to mitigate the shortcomings of the interleaved control.

3.1. Velocity Control Vector Definitions

With the definition for the truth-states of Eq. (1) in hand, a number of other important control vector quantities may also be derived. First, the imparted velocity estimate $\Delta\hat{\mathbf{v}}_c$ is defined as the expected value of the true velocity-change,

$$\Delta\hat{\mathbf{v}}_c(t_1,t_2) = E\left[\Delta\mathbf{v}_c(t_1,t_2)\right] \tag{2}$$

The maneuver knowledge-error ($\delta\tilde{\mathbf{v}}$) is the difference between the estimate and truth

$$\delta\hat{\mathbf{v}}(t_1,t_2) = \Delta\hat{\mathbf{v}}_c(t_1,t_2) - \Delta\mathbf{v}_c(t_1,t_2) \tag{3}$$

The true performance metric for the system is the control-error $\delta\mathbf{v}$, which is the difference between the commanded velocity-change (target) and the truth

$$\delta\mathbf{v}(t_1,t_2) = \Delta\mathbf{v}_c(t_1,t_2) - \Delta\mathbf{v}_{\mathsf{tgt}}(t_1,t_2) \tag{4}$$

Finally, the definition of the servo-error ($\delta\mathbf{v}_{\mathsf{servo}}$) is the difference between the target and estimate,

$$\delta\mathbf{v}_{\mathsf{servo}} = \Delta\mathbf{v}_{\mathsf{tgt}}(t_1,t_2) - \Delta\hat{\mathbf{v}}_c(t_1,t_2) \tag{5}$$

and is the quantity that the controller actively regulates.

3.2. Velocity Control

The ΔV controller follows the design principles of a classic tracker—with both a time-varying target, and velocity-estimate feedback. A predetermined velocity-change profile is uploaded to the spacecraft prior to each maneuver. The trajectory is in the form of a piece-wise linear look-up table—a ΔV in ECI J2000 versus spacecraft time. There are very few constraints on the nature of the profile. For example, it may be non-monotonically increasing in magnitude, and/or it may possess arbitrary spatial curvature. However, it must be constructed with care in the vicinity of the saturation limits of the thrusters or the system will perpetually lag behind the target—potentially failing to regulate the servo-error sufficiently within a given maneuver window. The controller is entirely responsible for the mapping of velocity commands—specified in the inertial frame—to the appropriate grouping of thrusters (i.e. "bank") capable of delivering an ideally torque-less translational force to the spacecraft. The projection of the servo-error into cylindrical coordinates determines if an axial or radial bank is a proper candidate for actuation.

3.2.1. Axial Control

On a spinning spacecraft, axially-aligned thrust is conceptually simpler. Since the spacecraft CM's radial offset from the spin axis is nominally zero, no torque balancing via pulse modulation is

attempted. However, since the axial thrust is always well aligned with the axial projection of servo-error, in order to reduce the amount of valve cycling and chattering between the top and bottom ($\pm$z) banks, the controller is designed to utilize a dynamic deadband, and limits commanding to roughly once every quarter spin period. During an axial control cycle, the control logic maneuvers the spacecraft towards a ΔV target corresponding to a time that is a quarter of a spin period in the future. This helps reduce integrated δv error although it's not an explicit requirement. Since translational and rotational control is interleaved (and translational control is given priority), this "packeting" of axial actuation also offers a potential benefit by freeing those thrusters for full momentum/attitude control. The qualifier "full" was applied to the previous statement because axial off-pulsing of a single thruster in a pair is also sometimes necessary—especially when a ΔV profile contains a dominant axial component and/or the (diaphragm-constrained) fuel mass is unbalanced about the spin axis.

3.2.2. Radial Control

The MMS radial thrusters are arranged in two banks of four, each directed along the positive and negative y-axis respectively. Pulse Width Modulation (on 8 Hz boundaries) of the upper or lower pairs in each quad facilitates torque balancing. This arrangement offers two opportunities per spin for thrust along a given inertially-fixed direction (roughly every 10-seconds). In order to avoid inducing directional error, the radial actuation is centered around the servo-error's projection in the spin plane. Because the controller tracks a time-varying velocity profile, the burn-centering problem is non-trivial. The precise timing affects the burn vector and vice versa—therefore an iterative solver is employed to resolve target centering down to a millisecond resolution. Explicitly, for a given servo-error, the current rate estimate can be used to predict the time at which the thrusters will align with the burn-arc center. However, at the predicted center-time, the target will have most likely shifted—resulting in a slightly different servo-error projection, *ad infinitum*. Fortunately, convergence is typically achieved within a few iterations.

Also, to prevent the controller from constantly lagging its target, a quarter spin period "look-ahead" strategy is employed. As shown in Fig. 5, this five seconds-of-time-bias keeps the servo-error straddling the velocity profile, and speeds up entry into a fine-tuning "trim" phase at the end of each maneuver. Similar to the axial control strategy, deadbands are employed to reduce the wasting of fuel due to chatter. During the "trim" phase, the deadband is reduced to allow the control to home in on the final target. Furthermore, instead of firing four radial thrusters at one time, a pair of radial thrusters are used to fine-tune the result.

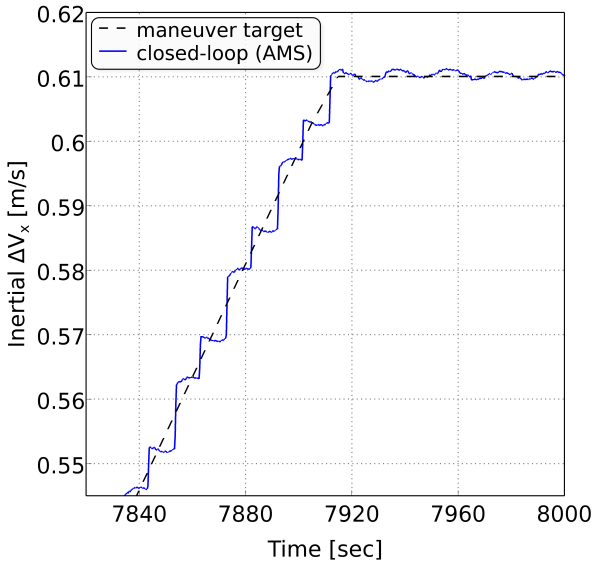

Figure 5. Velocity Controller Telemetry

3.2.3. Momentum Control

The spin axis inertial pointing direction is important to the MMS science instrument suite. For this reason, each observatory performs a momentum adjustment (ΔH) immediately following every ΔV. While the specifics of the ΔH control logic are not examined here (see [6]), it is also important to hold pointing, minimize nutation, and maintain spin during a ΔV maneuver (not only for the instruments, but also for accurate velocity estimation). Momentum control during a ΔV maneuver (DVDH) employs the same Lyapunov-based controller as the stand-alone ΔH mode, with two main differences—the off-pulsing of axial-thrusters, and the frequency of the control.

Off-pulsing Monte Carlo simulations exposed a shortcoming of the original DVDH design. When a target ΔV profile contains a dominant axial component, the axial thrusters may be busy tracking that velocity profile—making them unavailable for attitude control. If the induced angular rate error also happens to travel outside of the radial thrusters' torque authority, the attitude of the observatory could be left uncontrolled during the ΔV maneuver. This design flaw necessitates the implementation of off-pulsing of a single axial thruster in a pair in order to maintain full 6-DOF control authority during ΔV. As seen pictorially in Fig. 6 for an efficiency-angle of 16° (see [6]), the rate error (blue) only intersects with those two red *small circles* representing torque authorities of axial thruster torque pairs. Due to EVD hardware characteristics, the off-pulse resolution is limited by the 4Hz ACS control cycle. Monte Carlo analysis confirmed that this methodology is effective.

DVDH Actuation Frequency Solo ΔH maneuvers only actuate up to once every seven seconds. This wait time was optimally chosen based on extensive parametric studies where special attention was paid to post-maneuver multi-body dynamics settling characteristics—particularly for the SDP booms.

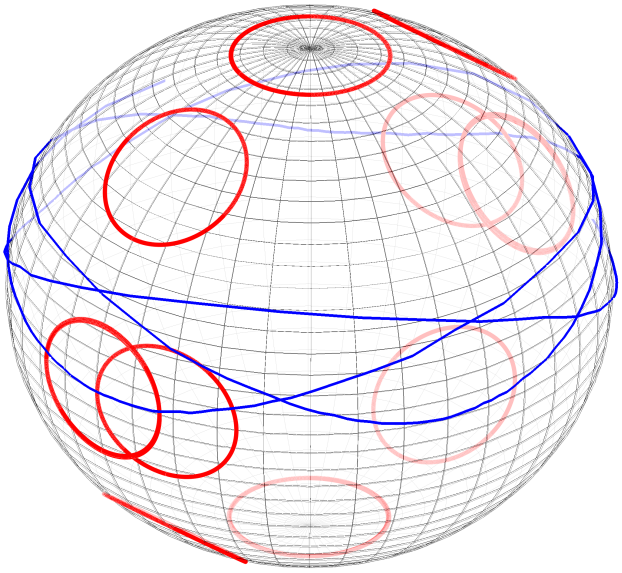

Figure 6. Control Coverage on Body Sphere

DVDH in contrast is allowed to actuate up to once every three seconds. Increasing DVDH actuation frequency seems to make up for the fact that it is given a lower priority than translational control (i.e. thrusters may not be available when needed). However, frequent DVDH actuation also tends to excite structural resonance with the two ADP booms. Three-second period was chosen as an acceptable balance between DVDH attitude control performance and avoiding ADP bending mode resonance.

4. System Robustness

Two major concerns of control system design are robustness in stability and performance in the presence of plant uncertainties. For MMS, exhaustive Monte Carlo simulations were used to address these twin concerns. Following the statistical methodology of Hanson and Beard[7], a 99%

confidence criteria (1% risk) was selected that permits zero failures for a sample size of 3410 runs.

This criteria was tested repeatedly using GSFC's *Freespace Simulation Environment* [8] to statistically vary over 250 model parameters—resulting in hundreds of thousands of time-domain simulations of maneuvers at full model fidelity. Figure 7 depicts one example of these results, and is annotated with the performance criteria used to determine execution-error acceptance for a formation maintenance class of closed-loop maneuvers (0-10 m/sec). The scatter plots of maneuver magnitude and directional error from 3500 runs shows ample margin versus the 3σ closed-loop (AMS) requirement (in cyan).

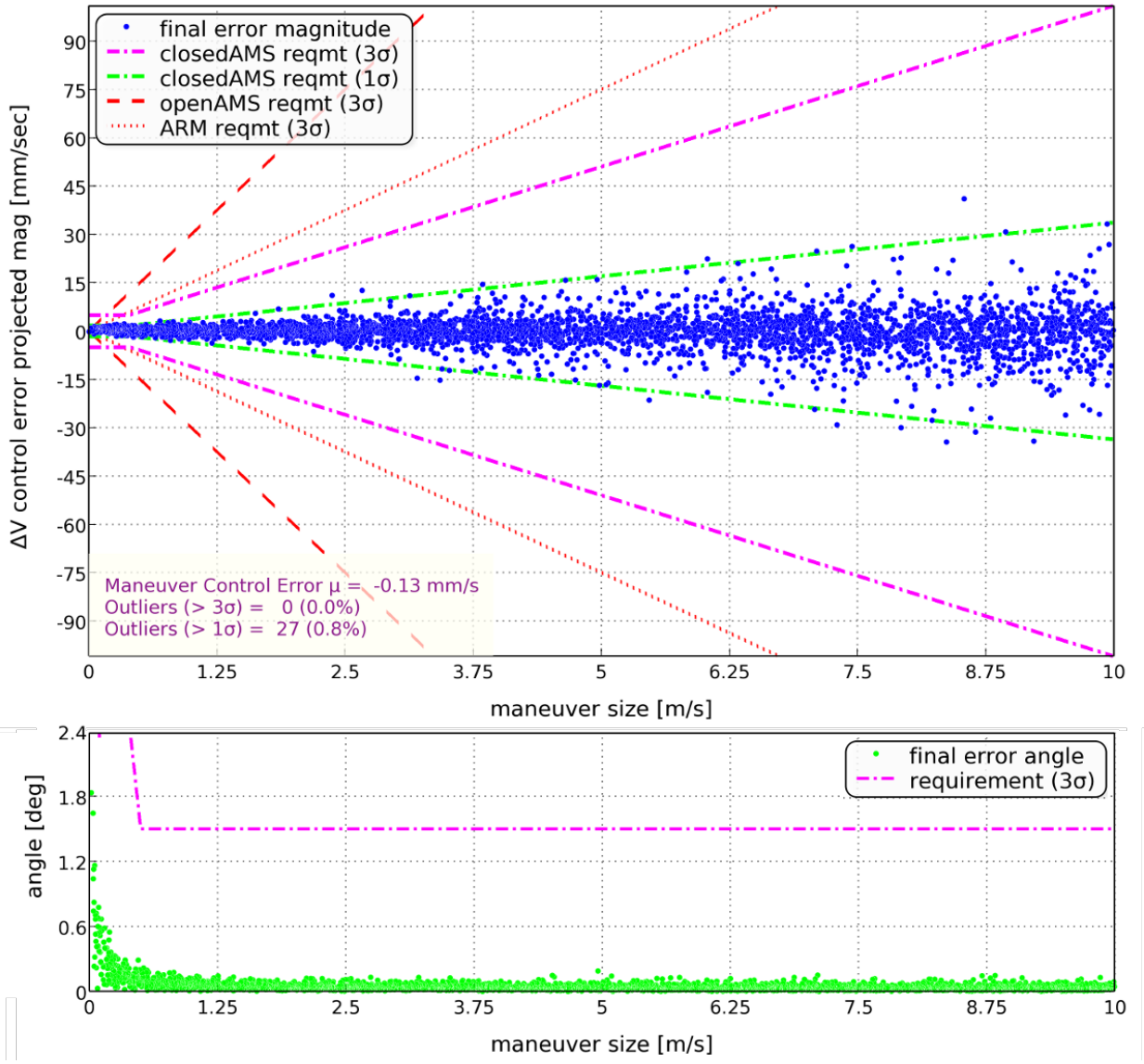

Figure 7. Monte Carlo Results for Formation Maintenance Maneuvers

5. MMS Mission Performance

MMS successfully initialized its 160 km tetrahedron formation for the first time on July 9th, 2015. Since then, MMS has performed the full formation maintenance maneuver sequence twice. The

initial formation tetrahedron lasted three weeks, the second formation tetrahedron lasted five, and the third formation is on track to last for at least two weeks. While it may still be early to conclude that the MMS system as a whole met the "maneuver at most once every two weeks on average" goal, it is a promising start.

5.1. On-orbit Calibrations and AMS Performance

A closer look at the on-orbit cumulative AMS data confirmed the pre-maneuver calibrations are effective in removing the combined effect of principal-axis uncertainty and AMS bias error. Figure 8 shows the on-orbit cumulative ΔV telemetry from the tail end of a principal axis calibration, to the beginning of a delta-V mode transition with data taken from a representative maneuver (FM140). After the principal-axis calibration, the on-board system picked up about 0.025 m/s of cumulative ΔV over the next 30 minutes. That is equivalent to integrating about 1.5 μg of bias. However, once the AMS bias calibration completes (at about 60 minutes before the maneuver starts), the slope became much more shallow. The on-board ACS only picked up about 1 mm/s of ΔV in the 60 minutes that followed. This not only confirms that the pre-maneuver calibrations was effective, it also substantiates the analytical assessment that the effect of integrating AMS noise is negligible. The AMS bias drift would have been a complicating factor, but it has proven to be very stable over a long period of time (see *AMS Bias Estimate* in Tab. 3).

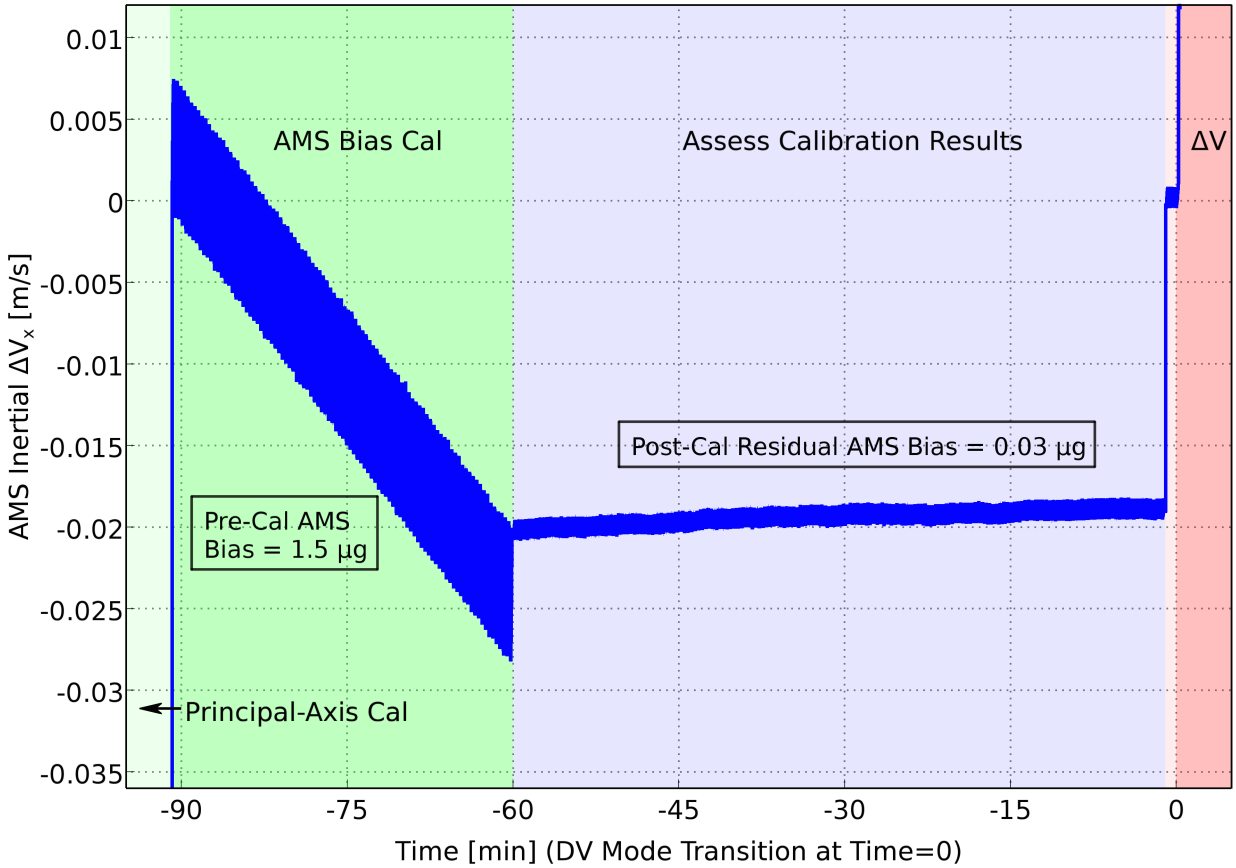

Figure 8. Pre-maneuver Calibration for MMS1 FM140

5.2. Closed-loop Maneuvers

The best avenue for determining the true closed-loop performance is through post-maneuver orbit determination. The GSFC-developed NAVIGATOR[9] Global Positioning System (GPS) hardware and GPS-Enhanced Onboard Navigation System (GEONS) software units are collectively providing real-time autonomous orbit determination with a record-breaking 5 meters (3σ) semi-major axis (SMA) accuracy[10]—operating effectively as high as 10 Earth radii. Beginning with the formation initialization maneuvers near the end of the MMS commissioning-phase, the following performance has been verified for the on-board orbital maneuvering system:

Table 3. On-Orbit Formation Maneuver Performance

Maneuver (DOY)	Obs ID	Final Target Magnitude	GEONS Solution Semi-major Axis Δ-error	Final Servo-Error		AMS Bias Estimate (μg)		
		mm/s		mm/s	% target	X	Y	Z
GS[1]-095 (166,167)	1	118.6	-1.14%	1.5	1.25%	114.7	78.9	49.6
	2	18.3	-0.57%	1.0	5.73%	94.3	93.9	47.3
	3	46.9	-0.73%	1.1	2.27%	75.2	92.5	140.1
	4	77.0	0.55%	1.1	1.44%	108.3	96.1	125.1
FI[2]-116 (188)	1	0	—	—	—	115.3	77.4	49.7
	2	4077.5	-0.79%	1.0	0.03%	95.0	94.0	47.5
	3	9175.6	-0.26%	0.2	0.00%	76.9	94.3	140.9
	4	4452.1	-0.26%	1.2	0.03%	107.2	93.9	125.4
FI-119 (190)	1	0	—	—	—	—	—	—
	2	3511.6	-0.61%	0.8	0.02%	93.7	94.0	47.6
	3	4149.7	-0.18%	1.3	0.03%	76.9	94.7	140.8
	4	6068.7	-0.27%	1.3	0.02%	106.9	95.5	125.3
FM[3]-139 (211)	1	1086.4	-0.70%	0.4	0.04%	114.3	77.1	49.4
	2	0	—	—	—	—	—	—
	3	0	—	—	—	—	—	—
	4	1714.3	0.08%	1.0	0.06%	107.1	98.4	125.8
FM-140 (211)	1	2688.5	0.41%	1.5	0.06%	114.5	77.3	49.2
	2	0	—	—	—	—	—	—
	3	0	—	—	—	—	—	—
	4	1259.2	0.27%	0.9	0.07%	106.8	98.6	125.8
FM-172 (243,244)	1	1369.6	0.04%	0.8	0.06%	114.6	76.8	48.8
	2	1008.1	-0.31%	1.5	0.15%	95.9	94.6	47.0
	3	2537.0	0.5%	1.2	0.05%	76.5	94.6	141.1
	4	0	—	—	—	—	—	—
FM-173 (244)	1	1406.9	-0.27%	0.8	0.06%	115.1	76.6	48.5
	2	748.8	-0.30%	0.4	0.05%	95.5	94.7	47.1
	3	1440.0	0.34%	1.1	0.08%	76.4	94.1	141.1
	4	0	—	—	—	—	—	—

While the error in targeted semi-major axis does not equate with controller error ($\delta\mathbf{v}$), SMA is directly linked to the orbital speed (e.g. the *vis-viva* equation). These early results (Tab. 3) indicate that the fleet is maneuvering successfully within the 3σ total mission requirements that are an amalgamation of ACS execution and flight dynamics planning errors. These results are particularly encouraging considering the sizes of the orbit stabilizing maneuvers (GS-095), since high percent accuracy is more challenging with small maneuvers. The sample mean $\bar{\mu}$ of these maneuvers is

[1]Orbit stabilizing maneuvers—executed by the controller in a manner identical to other formation maneuvers.

[2]Formation initialization maneuvers

[3]Formation maintenance maneuvers

-0.104%, with a sample standard deviation $\bar{\sigma}$ of 0.505%. Based on this relatively small sample size of 20 cases, we can state with a 90% confidence that the true standard deviation lies in the range of 0.401–0.692%, with the caveat that the distribution of maneuver errors is assumed Gaussian.

Ultimately, the criteria for a successful MMS maneuvering-system design will be the length of time for which a high-quality formation can be preserved—and that will be measured in the frequency of corrective maneuvers. This will be especially evident when the formation moves from its current average separation of approximately 160 km down to as little as 4 km.

6. Acknowledgments

We sincerely appreciate the efforts of Julie Thienel, Juan Raymond, Joseph Sedlak, Russell Carpenter, John Van Eepoel, Ken London, Scott Tucker, Conrad Schiff, and F. Landis Markley for numerous discussions during model development. ZIN Technologies went above and beyond expectations on the error analysis and testing of the AMS; their team leads included Alan Chmiel, James Bontempo, Gilead Kutnick and Melissa LaBarbera. Finally, we also need to thank the rest of MMS Team: Wendy Morgenstern, Oscar Hsu, Kathie Blackman, Shaun Oborn, Suyog Benegalrao, Lia Sacks, Blair Carter, Charles Campbell, Joel Gambino, Milton Davis, Ron Miller, Peter Kutt, Michael Yang, Stephen Mariconti, John Carro, and Josephine San for getting MMS to flight and making this work.

7. References

[1] Gramling, C. "Overview of the Magnetospheric Multiscale Formation Flying Mission." "Proceeding of the 2009 AAS/AIAA Astrodynamics Specialist Conference," Pittsburg, PA, October 2015. AAS 09-328.

[2] Long, A. "Navigation Operations for the Magnetospheric Multiscale Mission." "Proceeding of the 25th International Symposium of Space Flight Dynamics," Munich, Germany, October 2015.

[3] Queen, S., Chai, D., and Placanica, S. "Orbital Maneuvering System Design and Performance for the Magnetospheric Multiscale Formation." "AAS/AIAA Astrodynamics Specialist Conference," Vail, CO, August 2015. AAS 15-815.

[4] Queen, S. and Benegalrao, S. "A Kalman Filter for Mass Property and Thrust Identification of the Spin-Stabilized Magnetospheric Multiscale Formation." "25th International Symposium on Space Flight Dynamics ISSFD," Munich, Germany, October 2015.

[5] Raymond, J. C., Sedlack, J. E., and Vint, B. "Attitude Ground System for the Magnetospheric MultiScale Mission." "25th International Symposium on Spaceflight Dynamics," Munich, Germany, October 2015.

[6] Queen, S., Shah, N., Benegalrao, S., and Blackman, K. "Generalized Momentum Control of the Spin-Stabilized Magnetospheric Multiscale Formation." "AAS/AIAA Astrodynamics Specialist Conference," Vail, CO, August 2015. AAS 15-816.

[7] Hanson, J. M. and Beard, B. B. "Applying Monte Carlo Simulation to Launch Vehicle Design and Requirements Verification." "AIAA Guidance, Navigation and Control Conference," Ontario, Canada, August 2010. AIAA 2010-8433.

[8] Hughes, P. M. "NASA Goddard Space Flight Center FY 2006 Internal Research and Development Program." Tech. Rep. 2006-AR-V6, NASA/Goddard Space Flight Center, Greenbelt, MD, 2007.

[9] Bamford, W., Mitchell, J., Southward, M., Baldwin, P., Winternitz, L., Heckler, G., Kurishh, R., and Sirotzky, S. "GPS Navigation for the Magnetospheric Multi-Scale Mission." "Proceedings of the 22nd International Technical Meeting of The Satellite Division of the Institute of Navigation (ION GNSS 2009)," Savannah, GA, Sept 2009. Pp. 1447-1457.

[10] Farahmand, M. "Magnetospheric Multiscale Mission Navigation Performance Using the Goddard Enhanced Onboard Navigation System." "Proceeding of the 25th International Symposium of Space Flight Dynamics," Munich, Germany, October 2015.